RESPONSE OF ECOLOGICALLY-MEDIATED SHALLOW INTERTIDAL SHORE TRANSITIONS TO EXTREME HYDRODYNAMIC FORCING (RESIST)

Möller, I.[1], Bouma, T.J.[2], Brendel, M.[3], Brooks, H.[1], Cao, H.[2], Carr, S.[4], Chirol, C.[5], Christie, E.[1], Dennis, R.[2], Eggermond, A.[9], Evans, B.[1], Lustig, J.[3], Miranda-Lange, M.[6], Nolte, S.[3], Paul, M.[7], Reents, S.[3], Rolfe, C.[1], Royse, K.[8], Schoutens, K.[9], Spencer, K.[5], Temmerman, S.[9], Kudella, M.[6]

[1]Cambridge Coastal Research Unit, Department of Geography, University of Cambridge, United Kingdom, im10003@cam.ac.uk
[2]Royal Netherlands Institute of Sea Research (NIOZ), The Netherlands, tjeerd.bouma@nioz.nl
[3]Biocenter Klein Flottbek, University of Hamburg, Germany, stefanie.nolte@uni-hamburg.de
[4]Geography/Science, Natural Resources & Outdoor Studies, University of Cumbria, United Kingdom, simon.carr@cumbria.ac.uk
[5]School of Geography, Queen Mary University of London, United Kingdom, k.spencer@qmul.ac.uk
[6]Forschungszentrum Küste, University of Hannover, Germany, kudella@fzk.uni-hannover.de
[7]Ludwig-Franzius-Institut für Wasserbau, Ästuar- und Küsteningenieurwesen Leibniz Universität Hannover, Germany, paul@lufi.uni-hannover.de
[8]British Geological Survey, Nottingham, United Kingdom, krro@bgs.ac.uk
[9]Ecosystem Management Research Group, University of Antwerp, Belgium, stijn.temmerman@uantwerpen.be

ABSTRACT

This paper reports on the preliminary results from a true-to-scale flume experiment carried out to better understand plant and sediment responses, as well as their interactions, under extreme hydrodynamic forcing in shallow coastal salt and brackish water marsh settings. We report here on bed level changes under individual plant seedlings and denser plant arrangements transplanted from seed and field sites on the Scheldt estuary and on the response of vertically extracted sediment cores from two UK field sites with contrasting sediment characteristics and plant species occupying the surface. Due to the relatively recent completion of the experiment in addition to time-consuming, complex data processing and analysis methods more time is required before definitive quantitative results can be reported. Initial insights into the general behaviour of salt marsh sediments under horizontal and vertical wave-driven hydrodynamic forcing, however, confirm marsh surfaces to be highly stable structures, at least during extreme storm surge events.

1. INTRODUCTION

A climate change induced acceleration in sea level rise and accompanying altered patterns of storm occurrence are set to affect shores globally throughout and beyond the 21st Century. Both sea level and wave climate have been shown to be key controls on coastal wetland evolution (i.e. phases of initiation, growth/stability, and erosion). At the same time, coastal wetlands have been shown to act as important buffers against sea level rise (by sediment accretion) and extreme storms (by wave and surge attenuation)(Möller et al., 2014). However, the risk of erosion of coastal wetland surfaces under extreme storms is yet poorly understood (Spencer et al., 2016). This leads to the need to determine the relative stability of these surface types when exposed to events of varying magnitude, particularly in the most seaward pioneer vegetation zone. Identifying what types of species and artificial protective measures are most effective in reducing erosion / increasing stability in a particular hydrodynamic setting will help identify which coastal management interventions are likely to be most successful in preventing (or at least significantly delaying) the loss of these valuable natural coastal buffers in the face of climate/environmental change.

Salt marshes are increasingly valued for their role in coastal defence, as they reduce the impact of waves and erosion on shorelines and engineered coastal defences behind salt marshes (Beaumont et al., 2008). Yet the response of salt marsh margins to extreme hydrodynamic forcing is complex and currently not well understood. The response of salt marsh and adjacent tidal flat sediments to wave forcing is considerably more complex than that of sandy shores (Schuerch et al., 2019). This complexity arises largely due to (a) the large silt/clay fractions present and thus the cohesive nature

of the sediment involved and (b) the presence of (partially mobile) biological 'structures' (plants and other organisms) within and on the surface (Bouma et al., 2005).
NW European macro-tidal shores have a negligible variation in water depth over short (< 2 m) distances and water depths over the upper intertidal zone rarely exceed 2 m such that significant wave-induced bed stress can only occur during high wave energy events. Direct observations of vegetation and sediment surface response to storm wave energy is rare (Cahoon, 2006). Establishing the impact of storms through detailed studies 'before' and 'after' is inherently difficult given the unpredictability of such events and few if any studies have been able to measure wave conditions over upper tidal flat surfaces during storms. The types of hydrodynamic conditions that lead to erosion of natural coastal features such as salt marshes, and the damage salt marsh plants sustain under wave forcing, are thus not well known. However, until we have such knowledge, it will not be possible to predict the way in which the future morphology of these systems, and thus the degree of natural coastal protection that they will provide, will alter with sea level rise and climate change. These issues are particularly critical in the early stages of marsh establishment and growth.
What is of particular concern in this context is that, while dense vegetation has been shown to protect the sediment bed from wave induced erosion (Spencer et al., 2016) (Fig. 1A), evidence suggests that a sparse vegetation cover can act as an active agent enhancing, rather than reducing, bed erosion. Such erosion occurs through bed scour around individual plant stems in relatively sandy soils (Fig. 1B) and mechanical action of flexible plant components (Fig. 1c) (Bouma et al., 2009; Feagin et al., 2009; Koppel et al., 2005) .

Figure 1: Examples of vegetation effects on fine-grained shores. A: protection by dense canopy; B: low-density plant cover with scour around individual stems; C: active scour through *Salicornia* plant movement on an eroding tidal flat (UK East coast; photos: I Möller)

This project thus aimed to quantify:

(1) how extreme wave-forcing affects vegetation (both seedling survival of pioneer species and damage incurred by mature marsh plants);
(2) how (and to what extent) vegetation typically present in the salt marsh pioneer zone affects erosion under extreme forcing conditions;
(3) how vegetated salt marsh soils exposed in cliffs respond to high energy wave conditions;
(4) how novel artificial erosion protection / stabilisation methods may be used to protect seedlings as a restoration measure (see 1) and reduce erosion as a conservation measure (see 3).

Here, we report specifically on results relating to aims (2) and (3) and focus specifically on surfaces adjacent to *Spartina* plants. Strong morphodynamic feedbacks exist between hydrodynamic forcing and the morphological characteristics of the tidal flat to salt marsh transition zone. By focussing on the most seaward salt marsh pioneer zone, exposed established dense canopies, and artificial erosion protection, we address key questions on how to manage vegetated tidal flats into the future.

2. METHODS

To achieve the above aims, we set up five separate 'experimental treatment zones' in the large wave flume (Grosser Wellenkanal, GWK), Hannover, Germany (see Figure 2 for experimental set-up).

All zones were exposed to a range of hydrodynamic conditions and were replaced with replicate marsh surfaces after four days of exposure, with three such four-day periods of exposure conducted overall (i.e. three replicate sets of marsh surfaces were exposed). Zones consisted of surfaces representing:

(A) Seedling establishment: individual seedlings of three species with different structures and stem flexibility and different associated substrates: *Scirpus* spp, *Spartina* spp, and *Puccinellia* spp;
(B) Pioneer zone plant tussocks: different densities of full-grown plants of the above species;
(C) Pioneer zone plant tussocks with erosion protection: a range of erosion protection/stabilisation measures applied to pioneer zone seedlings (same species above);
(D) Dense canopy with fronting tidal flat: pioneer and higher marsh species of contrasting flexibility/stiffness (*Spartina* spp and *Elymus* spp) as dense canopy with flat sediment surface in front; and
(E) Clifflet zone: Dense *Spartina* canopy on 10 cm high clifflet and alternative sculpted transitions to bare sediment (control) as well as with erosion reduction measures applied.

In addition, several meters behind the horizontal test section, sediment cores were mounted with an open side facing the approaching waves. They were deployed fully submerged during replicate 1 and 2. For replicate 3 they were elevated such that the still water level was at the core centre. Cores were sampled at Warton and Tillingham Flats in the UK prior to the experiments and transported to GWK in chilled conditions by car. The cores from Warton are characterised by sandy sediment while the Tillingham samples are dominated by silty sediment.

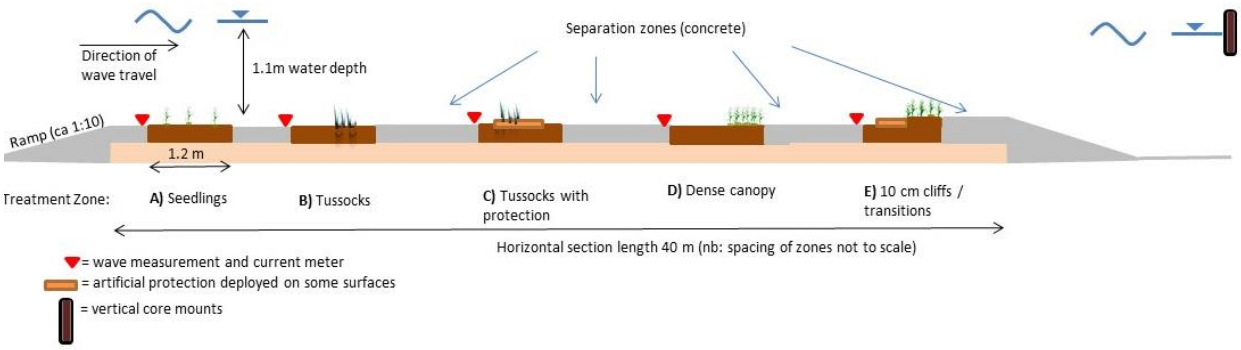

Figure 2: General setup of five experimental test sections and vertical core mount locations on cross-flume steel bar (nb: not to scale; zones A/B and C/D were swapped between wave runs 8 and 9)

Experimental Layout

A horizontal experimental platform was constructed on a sand base (Fig. 2), similar to that successfully deployed by Möller et al. (2014) in the GWK flume. The above zones stretched across the flume and consisted of 5 Europallets (0.8 x 1.2 x 0.3 m dimension, thus leaving a 0.5 m gap between the flume walls on either side and the marsh surfaces) with wooden frames. Each pallet was fully filled with substrate and transplanted seedlings or plant tussocks of varying arrangement according to zone layout excavated from sites in the Scheldt estuary. Fill sediment was flush with the sides of the wooden boxes and composed of 32% silt/clay (< 63 µm), and 31%, 11%, 24%, and 2% very fine, fine, medium, and coarse sand respectively. A previous experiment with similar material showed no significant edge-erosion effects at the juncture between soil and hard abutting surfaces (Möller et al., 2014). The particle size distribution and shear strength of the fill sediment compares well with sediments found on north-west European salt marshes and tidal flats (see Table 1). With three replicates for replacement after each four days of flume-generated wave conditions, a total of 75 pallets were prepared in this way. Pallets were carefully transported into the flume by crane, after positioning them in their final zone layout on solid steel sleepers, such that no stress was placed on the soil surfaces prior to experimental wave runs.

Each of the replicate sets of pallets was exposed to one wave condition per day over the course of four days (Table 2) after which the replacement set of pallets was deployed. Wave conditions on day 1, 5, and 9 thus represent the first wave exposure of each of the three sets of replicates. Subsequent exposures to waves (on day 2-4, 6-8, and 10-12) then affected soils and plants that had already been affected at least once by prior conditions, although soil elevation change measurements took place before and after each wave run (see below).

Table 1: Fill sediment used in flume experiment compared to sediment at four salt marsh locations

Sediment source	Shear strenghth (kg/cm^2)		Mean size (µm)	% silt/clay (< 63 µm)
	Mean	Range		
Fill sediment (this experiment)	4.72	3.4-6.8	152.02	32.25
Tillingham, UK	4.56	0.8-9.6	70.26	73.16
Warton, UK			92.05	39.43
Zuidgors, NL	3.59	2.5-4.2		
Waarde, NL	4.81	4.1-5.5		
Rillard, NL	4.34	3.9-4.9		
Rattenkaai, NL	3.87	2.7-4.7		

Table 2: Wave conditions applied to all zones as forced by the wave maker during the three sets of simulations applied

	Wave run set S1				Wave run set S2				Wave run set S3			
Treatment set	Replicate 1				Replicate 2				Replicate 3			
Wave condition	1	2	3	4	5	6	7	8	9	10	11	12*
Hs (m)	0.3	0.40	0.6	0.7	0.7	0.7	0.8	0.8	0.7	0.8	0.8	0.5
Wave Period (s)	2.5	4.1	3.6	5.5	3.9	3.9	5.8	5.8	3.9	5.8	5.8	6.0

*monochromatic waves were run on this last day

To avoid the along-flume position of zones systematically affecting their wave exposure, zones C and D were swapped with zones A and B at the start of week 3 of the experiment, and wave conditions 6-8 were re-run as conditions 9, 10, and 11, with these zones in different positions within the flume.

Hydrodynamic measurements

Near-bed currents and waves were recorded immediately in front of each experimental zone using Accoustic Doppler Velocimeters (ADVs) mounted at a height of 15 cm above the concrete platform in the centre of the flume and flume wall mounted wave gauge arrays. With the exception of the final day of wave runs (wave condition 12), when monochromatic waves of the highest near-breaking condition were generated, waves were randomly generated in series of ca 1000 waves matching North Sea conditions (JONSWAP spectrum). Observed maxima/minima and mean forward and return wave currents alongside wave height and period were derived from the high-frequency (100 Hz) ADV measurements and wave gauge water level time-series. Wave reflection was negligible as determined using an array of three wave gauges in front of and behind the experimental platform.

Pre- and post-exposure bed elevation measurements

In addition to laser scanned bed levels, manual bed-level changes were recorded with a sedimentation-erosion table placed on fixed mounts on the concrete platform to provide locational accuracy (similar to the method described in Spencer et al.[2]) (Figure 3). The manual measurements allowed bed-level change to be determined at 27 locations per pallet (9 locations evenly spaced along 3 along-flume rows) at millimetre accuracy.

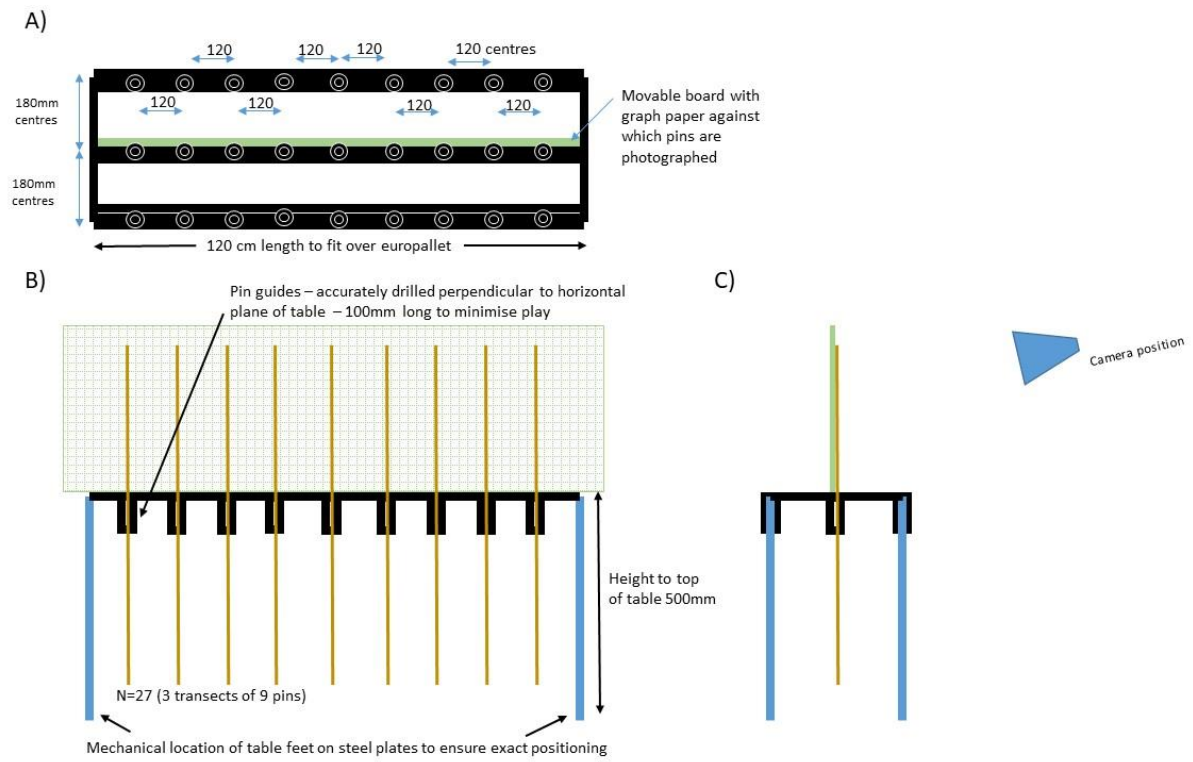

Figure 3: Manual bed-level measurements via purpose designed sedimentation/erosion table; A) top-down view of 27 pin locations positioned on three long-axis bars, B) side-view of pins and tops of pins against graph paper for quick deployment and subsequent transcribing from photographs, and C) view along the flume with pins inserted in central row.

3. RESULTS

Hydrodynamic forcing conditions

Wave heights and wave periods in the first week (Figure 4) produced a steady increase in mean and maximum wave-induced bed velocities (U_{max}), with some along-flume variability due to wave instabilities introduced as waves travelled over the test section (Figure 5). Maximum instantaneous currents were particularly variable (Figure 5B), with the highest currents overall reaching 2.33 ms^{-1} at the front of the platform during test no. 7. The average simulated random wave conditions were almost identical between test no. 7 and 11 (Hs of 0.73 and 0.72 m respectively, and Tp of 5.6 for both). The third replicate set of pallets in the front zone, however, experienced a much larger maximum stress than the second replicate on the third day of exposure (2.33 ms^{-1} compared to 0.89 ms^{-1}). As pallets were swapped between zones A/B and C/D when deploying the third replicate set of pallets, it was the plant tussock zone that experienced these conditions (see also Figure 2).

Bed level responses

Soil surface response to the hydrodynamic stress simulated in these extreme wave conditions was minimal, with average bed level change not exceeding 4 mm and both positive and negative bed level changes observed. The SET pin methodology resulted in n = 27 individual point measurements per pallet and variability of bed level change measured was high, with standard deviations larger than the average recorded bed level change per pallet.

There is no clear pattern of mean per-pallet bed level response to the applied hydrodynamic forcing and the greatest mean surface elevation changes occurred under conditions in which currents exceeded 0.8 ms^{-1} (i.e. after wave run 3) for most pallets that contained tussocks or dense canopies. Standard deviations are high and span zero change for all but two wave conditions applied to the *Spartina* seedling pallets: during the first wave run (maximum bed velocities 0.36 ms^{-1}) and test no. 11 (maximum bed velocities 1.21 ms^{-1}).

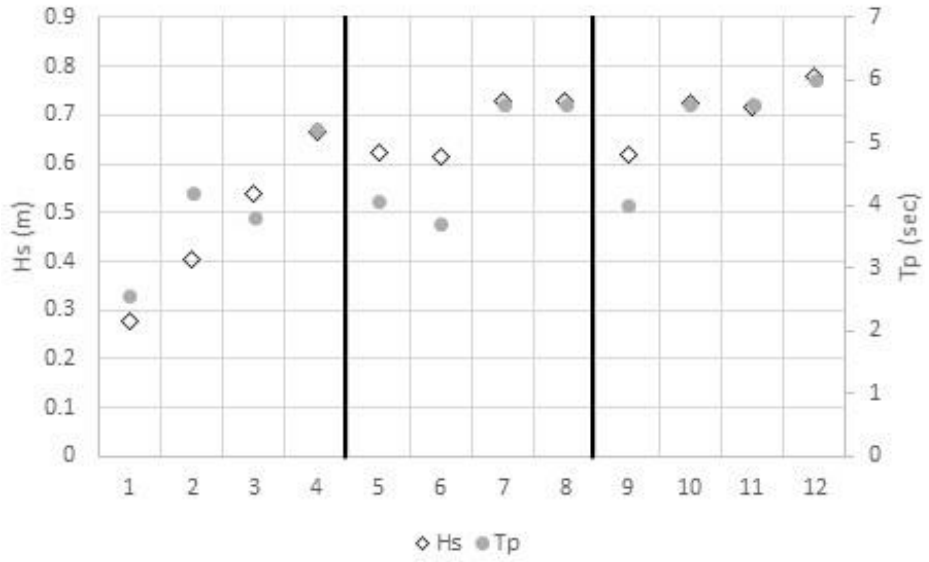

Figure 4: Significant wave height (Hs) and peak wave periods (Tp) as recorded immediately fronting the first zone (A) (nb: x-axis numbers represent exposure (day) number and exposure/day 12 conditions consisted of monochromatic waves); black lines indicate changeover of replicate pallet sets

In the case of the pallets planted with tussocks of *Spartina*, a tendency towards greater bed level change can be observed for the third replicate. They were exposed to current maxima exceeding 1 ms^{-1}, compared to the previous two, which were exposed to < 1 ms^{-1} on their first day of inundation (Figure 5B) . In addition, they were positioned in zones A and B during this replicate, which experienced higher current maxima than zones C and D where they were located during replicate one and two.

Overall, pallets covered with a dense canopy and/or cliff and fronting unvegetated soil showed comparatively higher variability in mean bed level change between consecutive wave runs and replicate pallet sets than those into which individual seedlings were planted. As mentioned above, however, per-pallet mean bed level changes overall were small compared to the variability amongst the 27 per-pallet pin measurements.

Vertical soil core responses

Figure 6 shows changes to the protrusion of the front face for both core types during replicate 2 exposure. During replicate 1 and 2, cores were fully submerged leading to higher velocities corresponding to areas of the core face located closer to the water level. For replicate 3, where still water level was at the midpoint of the core, the mean maximum velocities decrease above and below a maximum located just above still water level as a consequence of fewer waves reaching the higher portions of the core. The vertical soil cores showed a clear difference in response to the first exposure for each of the three replicates as well as between the two different extraction sites. Both cores behaved relatively similarly, with < 2 mm change along the length of the core during the first exposure, where mean orbital velocities remained below 0.1 ms^{-1} along the entire front face of the core. The second replicate set of cores exposed for the first time in run 5 , however, showed a clear difference in behaviour, particularly towards the top third of the core. In this run, orbital velocities exceeded 0.26 ms^{-1} along the length of the core, with > 0.28 ms^{-1} achieved at the top of the exposed core faces. The different sediment types responded differently to the wave forcing with the sandier core from Warton exhibiting sediment loss towards the top of the core which increased under the changed inundation level during replicate 3. The clay-rich cores from Tillingham Flats, on the other hand, even exhibited protrusion towards the top of the core for both inundation depths.

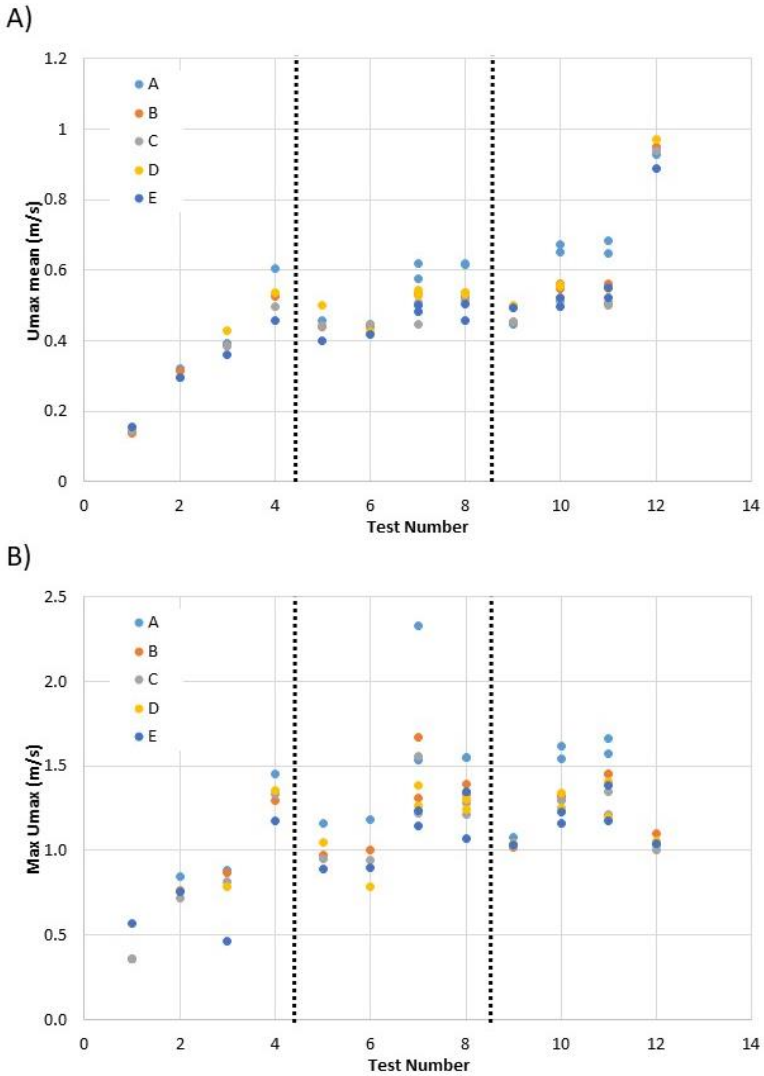

Figure 5: Mean (A) and maximum (B) wave-induced currents in the direction of wave travel for all 12 wave runs (see also Table 1 and Figure 4 for wave conditions); stippled lines indicate changeover of replicate pallet sets (nb: run number 12 consisted of monochromatic waves). Letters indicate zones at which the measurements were taken.

4. DISCUSSION

Response of horizontal surfaces to hydrodynamic forcing

The hydrodynamic forcing at the bed generated in this experiment exceeds that reported in other flume and field studies for comparable water depths. In Maza et al.'s (2015) large-scale experiment on wave damping by vegetation, for example, wave plus current generated velocities do not exceed 0.3 ms^{-1}. In the field, Shi et al. (2016) report velocities of just below 0.3 ms^{-1} from the upper tidal flats of the Jiangsu coast of China and Le Hir et al. (2000) report tidally driven maximum velocities of around 0.45 ms^{-1} on the Brouage mudflat, France. For the same location, Le Hir et al. (2000) suggest maximum wave-induced bed shear stress is achieved on the upper tidal flat at mid-tide level when the 'saturation' wave height is achieved, i.e. at the point at which the wave height to water depth ratio reaches its maximum, a value of 0.15 on the Brouage tidal flat. Wave height to water depth ratios in this experiment exceeded this value by some margin (> 0.26 in all wave runs), thus bed stresses would have far exceeded those observed in the field. The second and third replicate set of pallets deployed in the flume experienced bed velocities that, at > 1 ms^{-1}, clearly far exceeded these reported values from the literature.

The low per-pallet mean response of bed elevation to any of the wave runs and the high variability in bed level changes within each pallet (the maximum mean per-pallet bed level change observed was 3 mm with a standard error of +/- 13) suggests that no spatially uniform or consistent lowering of bed levels took place during the individual experimental runs.

Figure 6: Impressions of the vertical soil core faces before (left) and after (right). Top: sandy sediment from Warton (right); Bottom: clay-rich sediment from Tillingham (replicate 2 prior to exposure (left) and after exposure to conditions 5-8 (right)) (nb: structures from the slicing clearly visible in both)

Response of vertical core faces to hydrodynamic forcing

The two types of cores extracted from the field differed most clearly in terms of their sedimentology and vegetation growth. The greater responsiveness of the core from Warton (WS) compared to that of Tillingham (TF) when exposed to waves in the flume may thus be the results of either or both the lower cohesion / coarser grain size and/or the presence of the salt marsh grass *Puccinellia* with its fine root system instead of the more woody *Atriplex* shrub. The fact that the difference between the cores was markedly greater towards the top half of the core in spite of relatively small differences in wave driven orbital velocities with elevation, however, suggests that the vegetation may have been the dominant influence. This result can be seen in the context of other studies, e.g. Feagin et al. (2009), who suggested that roots protruding from exposed marsh cliffs can act as mechanical agents of erosion under wave action. Here, however, it is likely, that this mechanical action was assisted by the relatively less cohesive (and thus more porous nature) of the soil matrix, allowing material to be more easily 'washed out' from between the dense filamentous root mat that characterises this type of vegetation.

5. CONCLUSION

Improved knowledge of the stability of intertidal coastal habitats is not only an important consideration for flood and erosion prevention under climate change, but is essential for the successful conservation of these highly ecologically valuable ecosystems in their own right.

This paper provides the first in a series of analyses of the results of our large-scale flume experiment. It is clear from the results presented that the lack of larger spatial patterns of bed-level

response to wave forcing apparent from the 27 pin readings within each pallet requires a finer spatial scale analysis of morphological change. Over the coming months we will conduct a more comprehensive analysis of the full results of bed level change derived from the deployment of a laser scanner and structure from motion photography. This should shed valuable insights into the highly spatially variable patterns of behaviour in response to the presence of different plant species and arrangements of plants within each pallet.

Our experiment has already, however, provided further proof alongside that of prior studies (e.g. Spencer et al., 2015), that exposed horizontal and vertical sedimentary surfaces typical of wetland-dominated intertidal shores are particularly resistant to wave forcing applied during single, extreme, inundation events. This in turn suggests that the importance of such individual events in terms of influencing the morphodynamic trajectory of salt marsh fringes is relatively low. We thus call for a re-evaluation of the role of extreme events versus more frequent events characterised by lower wave energy in terms of forcing morphological change.

ACKNOWLEDGEMENT

This project has received funding from the European Union's Horizon 2020 research and innovation programme under grant agreement No 654110, HYDRALAB+. The University of Cambridge team members acknowledge funding from the Natural Environment Research Council (Response of Ecologically-mediated Shallow Intertidal Shores and their Transitions to extreme hydrodynamic forcing in UK settings (RESIST-UK), Ref: NE/R01082X/1, and Physical and biological dynamic coastal processes and their role in coastal recovery (BLUE-coast), Ref: NE/N015878/1).

REFERENCES

Beaumont, N. J., Austen, M. C., Mangi, S. C., and Townsend, M. (2008). Economic valuation for the conservation of marine biodiversity. *Mar. Pollut. Bull.* 56, 386–396. doi:10.1016/j.marpolbul.2007.11.013.

Bouma, T. J., De Vries, M. B., Low, E., Kusters, L., Herman, P. M. J., Tánczos, I. C., et al. (2005). Flow hydrodynamics on a mudflat and in salt marsh vegetation: Identifying general relationships for habitat characterisations. *Hydrobiologia* 540, 259–274. doi:10.1007/s10750-004-7149-0.

Bouma, T. J., Friedrichs, M., Klaassen, P., van Wesenbeeck, B. K., Brun, F. G., Temmerman, S., et al. (2009). Effects of shoot stiffness, shoot size and current velocity on scouring sediment from around seedlings and propagules. *Mar. Ecol. Prog. Ser.* 388, 293–297. doi:10.3354/meps08130.

Cahoon, D. R. (2006). A Review of Major Storm Impacts on Coastal Wetland Elevations. *Estuaries and coasts* 29, 889–898.

Feagin, R. A., Lozada-Bernard, S. M., Ravens, T. M., Möller, I., Yeager, K. M., and Baird, a H. (2009). Does vegetation prevent wave erosion of salt marsh edges? *Proc. Natl. Acad. Sci. U. S. A.* 106, 10109–13. doi:10.1073/pnas.0901297106.

Koppel, J. Van De, Wal, D. Van Der, Bakker, J. P., and Herman, P. M. J. (2005). Self-organization and vegetation collapse in salt marsh ecosystems. *Am. Nat.* 165, E1–E12.

Le Hir, P., Roberts, W., Cazaillet, O., Christie, M., Bassoullet, P., and Bacher, C. (2000). Characterization of intertidal flat hydrodynamics. *Cont. Shelf Res.* 20, 1433–1459. doi:10.1016/S0278-4343(00)00031-5.

Maza, M., Lara, J. L., and Losada, I. J. (2015). Tsunami wave interaction with mangrove forests: A 3-D numerical approach. *Coast. Eng.* 98, 33–54. doi:10.1016/j.coastaleng.2015.01.002.

Möller, I., Kudella, M., Rupprecht, F., Spencer, T., Paul, M., van Wesenbeeck, B. K., et al. (2014). Wave attenuation over coastal salt marshes under storm surge conditions. *Nat. Geosci.* 7, 727–731. doi:10.1038/ngeo2251.

Schuerch, M., Spencer, T., and Evans, B. (2019). Coupling between tidal mudflats and salt marshes affects marsh morphology. *Mar. Geol.* 412, 95–106. doi:10.1016/j.margeo.2019.03.008.

Shi, B., Yu, Q., Gao, S., Wang, Y. P., and Wang, Y. (2016). Physical and sedimentary processes on the tidal flat of central Jiangsu Coast, China: Headland induced tidal eddies and benthic fluid mud layers. *Cont. Shelf Res.* 133, 26–36. doi:10.1016/j.csr.2016.12.015.

Spencer, T., Möller, I., Rupprecht, F., Bouma, T. J., van Wesenbeeck, B. K., Kudella, M., et al. (2016). Salt marsh surface survives true-to-scale simulated storm surges. *Earth Surf. Process. Landforms* 41, 543–552. doi:10.1002/esp.3867.